ADVANCED ENERGY MATERIALS
www.advmat.de

Macromolecular Scaffolding: The Relationship Between Nanoscale Architecture and Function in Multichromophoric Arrays for Organic Electronics

By *Vincenzo Palermo,* Erik Schwartz, Chris E. Finlayson, Andrea Liscio, Matthijs B. J. Otten, Sara Trapani, Klaus Müllen,* David Beljonne,* Richard H. Friend,* Roeland J. M. Nolte, Alan E. Rowan,* and Paolo Samorì**

The optimization of the electronic properties of molecular materials based on optically or electrically active organic building blocks requires a fine-tuning of their self-assembly properties at surfaces. Such a fine-tuning can be obtained on a scale up to 10 nm by mastering principles of supramolecular chemistry, i.e., by using suitably designed molecules interacting via pre-programmed noncovalent forces. The control and fine-tuning on a greater length scale is more difficult and challenging. This Research News highlights recent results we obtained on a new class of macromolecules that possess a very rigid backbone and side chains that point away from this backbone. Each side chain contains an organic semiconducting moiety, whose position and electronic interaction with neighboring moieties are dictated by the central macromolecular scaffold. A combined experimental and theoretical approach has made it possible to unravel the physical and chemical properties of this system across multiple length scales. The (opto)electronic properties of the new functional architectures have been explored by constructing prototypes of field-effect transistors and solar cells, thereby providing direct insight into the relationship between architecture and function.

1. Introduction

The physicochemical properties of organic (multi)component films for optoelectronic applications depend on both the mesoscopic and nanoscale architecture within the semiconducting material.[1] Two main classes of semiconducting materials are commonly employed: polymers and (liquid)-crystals of small aromatic molecules. Whereas polymers (e.g. polyphenylenevinylenes and polythiophenes) are easily solution-processable in thin and uniform layers,[2] small molecules can form highly defined (liquid)-crystalline structures featuring high charge mobilities.[3]

The self-assembly of π-conjugated (macro)molecules at surfaces forming highly ordered supramolecular architectures has been widely explored in the last two decades.[4] Through the proper design of side-functionalities attached to the conjugated backbone, it has been possible to control the self-assembly at the 1–10 nm scale. This was accomplished by the synthesis of molecular systems undergoing recognition events through a variety of noncovalent interactions.[5] To expand the control to conjugated assemblies at larger length scales, strategies involving extrinsic forces have been proposed. This includes the use of pre-patterned surfaces,[6] hydrodynamic forces,[7] and electric[8] or magnetic fields.[9] The involved procedures are, however, often cumbersome and the parameters vary from system to system.

We have recently devised a practical protocol for achieving a full control over the position of functional molecular units in 2D on a scale up to some hundreds of nanometers. This strategy relies on the use of a rigid polymeric scaffold, i.e., a structurally

[*] Dr. V. Palermo, Dr. A. Liscio
Instituto per la Sintesi Organica e la Fotoreattività
Consiglio Nazionale delle Ricerche, Via Gobetti 101
40129 Bologna (Italy)
E-mail: palermo@isof.cnr.it
Prof. K. Müllen
Max-Planck Institute for Polymer Research
Ackermann 10, 55124 Mainz (Germany)
E-mail: muellen@mpip-mainz.mpg.de
Dr. D. Beljonne, S. Trapani
Université de Mons-Hainaut, Place du Parc 20
7000 Mons (Belgium)
E-mail: david@averell.umh.ac.be

DOI: 10.1002/adma.200903672

[*] Prof. R. H. Friend, Dr. C. E. Finlayson
Cavendish Laboratory, University of Cambridge
J. J. Thomson Avenue Cambridge CB3 0HE (UK)
E-mail: rhf10@cam.ac.uk
Prof. A. E. Rowan, E. Schwartz, M. B. J. Otten, Prof. R. J. M. Nolte
Institute for Molecules and Materials
Radboud University Nijmegen
Heyendaalseweg 135, 6525 AJ Nijmegen (The Netherlands)
E-mail: a.rowan@science.ru.nl
Prof. P. Samorì
Nanochemistry Laboratory, ISIS, Université de Strasbourg and CNRS (UMR 7006), 8
allée Gaspard Monge
67000 Strasbourg (France)
E-mail: samori@unistra.fr

Vincenzo Palermo received his Ph.D in physical chemistry in 2003 at the University of Bologna. After working at the University of Utrecht (the Netherlands) and at NRC, Ottawa (Canada), he is now researcher at ISOF in Bologna, where he is responsible of the Nanochemistry lab and coordinator of the research unit ''Functional Organic Materials for High-Tech applications''. His present research interests are in the self-assembly and nanoscale electrical characterization of materials for optoelectronics.

Alan Rowan studied at the University of Liverpool, England, where he obtained a BSc 1st Honours in Chemistry and then a PhD in Physical Organic Chemistry. In 1992 he moved to New Zealand where he completed a Post doctoral study in the field of Supramolecular chemistry with Prof C. Hunter. In 1994 he moved to Nijmegen the Netherlands as a Mare Curie Fellow, and then as Assistant and Associate Professor with Prof R.J. Nolte. In 2005, he set up a new department of Molecular Materials in the Institute for Molecules and Materials, Nijmegen. His interests are in the relationship between molecular architecture and function, in self-assembling and macromolecular (bio)-organic and magnetic materials.

Paolo Samorì (Imola, Italy, 1971) is full professor at the Institut de Science et d'Ingénierie Supramoléculaires of the Université de Strasbourg. In 2000 he received his Ph.D in Chemistry from the Humboldt University Berlin. From 2001 to 2008 he was permanent research scientist at ISOF-CNR Bologna. His research interests include the application of scanning probe microscopy beyond imaging, hierarchical self-assembly of hybrid architectures at surfaces, supramolecular electronics, and the fabrication of molecular-scale nanodevices.

well-defined nano-object, which is employed as a backbone upon which functional groups can be exactly positioned. In this way the interaction between the functional groups can be fully controlled from the sub-nanometer up to the few hundreds of nanometers scale.

The scaffold that we have designed and synthesized is a poly(isocyanide) derivative bearing L-alanine-D-alanine methyl ester side groups (**LD-PIAA**) (Fig. 1a).[10] In 2002 we demonstrated that such a polymer is extremely rigid and possesses a persistence length of at least 76 nm, being as stiff as double stranded DNA.[11] This high rigidity is due to the 4_1 helical backbone of the polymer and the hydrogen bonding network formed between the pendant alanine side-chains (Fig. 1b). The synthetic versatility of this macromolecular system allows the controlled functionalization of the side-chains with a broad arsenal of moieties.

We are particularly interested in electrically and optically active π-conjugated systems for optoelectronic applications such as LEDs,[2,12] field-effect transistors,[13] light-emitting transistors,[14] flexible displays,[15] and solar cells,[16] in which the control over the architecture is critical for the properties of the material and the device, in particular on its performance.

In this connection we have chosen as prototypical functional system the perylenebis(dicarboximide) (**M-PDI**) group,[17] which is a well-known n-type semiconductor and of interest as active component in the fabrication of field-effect transistors (FETs)[18] and solar cells.[19,20]

2. Synthesis, Solution Processing and Modeling

We have developed different synthetic strategies to covalently attach a **M-PDI** group to the side-chain of the polyisocyanide backbone. The PDI appended polymers are prepared by a nickel catalyzed polymerization reaction of the isocyanide monomers **M-PDI-1** and **M-PDI-2** (Fig. 1).[21] Polymer **P-PDI-2**, has bulky phenoxy groups in the bay area of the PDI and this feature can be expected to hinder the tendency of PDIs to stack through π–π interactions. Polymer **P-PDI-1** bears long alkyl tails in its side chains to increase the solubility of the compound in organic solvents. The polymers were soluble in chlorinated solvents (CH_2Cl_2, $CHCl_3$, dichloroethane, tetrachloroethane) and other solvents such as benzene, toluene and tetrahydrofuran. From IR spectroscopy studies, i.e., from the disappearance of the isocyanide signal at 2140 cm^{-1}, it was determined that the polymerization reaction was complete after ~15 min. Upon polymerization the IR-absorptions at 3438 and 3391 cm^{-1}, attributed to the *trans* and *cis* amide N–H stretching vibrations, respectively, shifted to 3294 cm^{-1}. This shift is indicative of hydrogen bond formation between the amide functions in the side chains as also observed for **LD-PIAA** (Fig. 1). Atomic Force Microscopy (AFM) images of the polymers revealed an average contour length of 180 nm for **P-PDI-1** and 110 nm for **P-PDI-2**, which corresponds to M_n's in the order of 10^5–10^6 g mol^{-1}.

The versatility of this synthetic strategy has been demonstrated through the syntheses of polyisocyanides exposing other chromophores, such as porphyrins[22] and thiophenes.[23] A more modular approach, which involves the post-modification of a polyisocyanide scaffold, relies on the use of the well-established click-chemistry approach.[24] A polymer scaffold with two alanine groups in its side chain and a terminal acetylene functionality,[25] was synthesized and (co)-clicked with a variety of azides leading to, for the first time, chromophoric water-soluble polyisocyanopeptides.[26] The wide variety of available azides allows the synthesis of a vast array of functionalized polymers with varying properties.

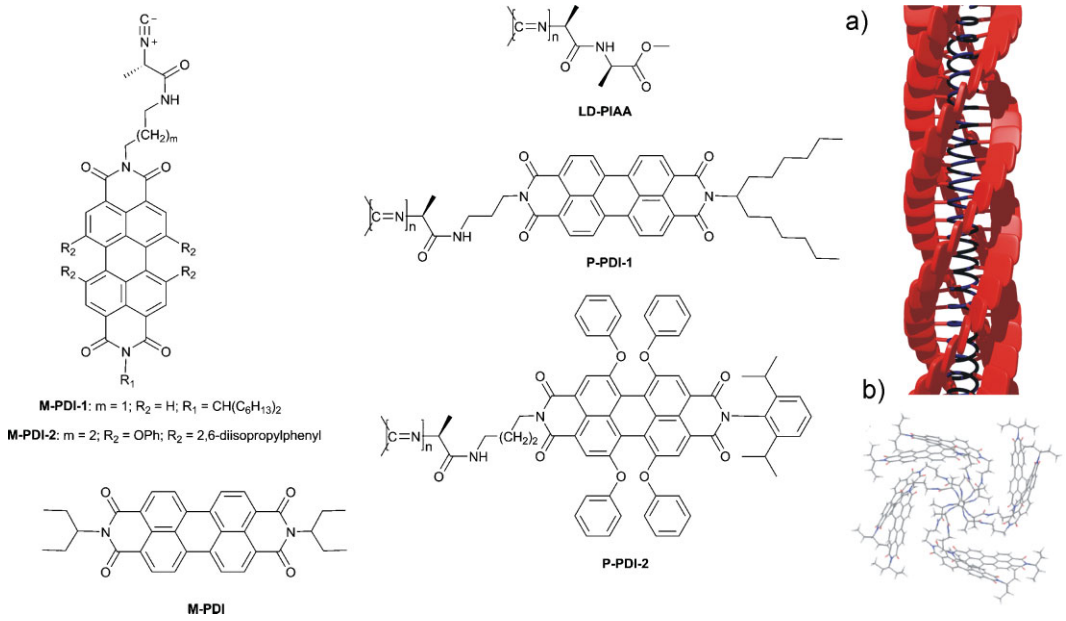

Figure 1. Molecular formulae, and a) helical motif of a **P-PDI**. b) Molecular modeling and spectroscopic studies suggest that **P-PDI-1** adopts a right-handed helix with ~3.75 repeat units per turn and edge-one interactions between the chromophores.

Spectroscopic analyses and extensive molecular dynamics studies on **P-PDI-1** revealed a well-defined 4_1 helix in which the PDI moieties form four ''helter-skelter-like'' overlapping pathways along which excitons and electrons can be predicted to rapidly migrate. Quantitatively, molecular dynamics (MD) simulations at room temperature have yielded electronic transfer integrals with an average value of 350 cm^{-1}. Compared to single crystals of small molecules such as the oligoacenes,[27] this is a significantly large value that should allow for efficient intramolecular electron transport along the polymer direction. The sizeable transfer integrals arise from the close packing of the PDI units and commensurate electronic coupling. The well-defined polymer scaffold is stabilized by hydrogen bonding arrays in the four side chains, to which the chromophores are attached, accounting for the precise architectural definition, and molecular stiffness observed for these compounds. MD studies showed that the chirality present in the polymer side chains is expressed in the formation of stable right-handed helices. The formation of chiral supramolecular structures is further supported by the observed and calculated bisignated Cotton effects. The structural definition of the chromophores aligned in one direction along the polymer backbone is highlighted by the extremely high exciton migration rates, as demonstrated experimentally. In particular, polarization-sensitive transient absorption measurements on **P-PDI-1** showed that the anisotropy in photo-induced absorption decays on timescales of the order of picoseconds, which is faster than in other studied π-conjugated polymers, such as polythiophene.[28] These rapid depolarization processes are due to the compact helical structure,[29] which promotes rapid exciton migration along the chiral arrangement of perylene stacks. In addition, high fractional changes in optical density (above ca. 1% in solution) are observed at short times after photo-excitation, as measured with transient absorption spectroscopy, showing an extremely high charged-excitation density on chains.

Overall, these multichromophoric arrays are unique as they combine an ultra-stiff central polymer main-chain scaffold along which the PDI chromophores can self-organize through π–π stacking, and polymer processability making them interesting and versatile nanowires for electronic devices.

3. Morphology at Surfaces

The assembly behavior of the polyisocyanides at surfaces has been explored with AFM by comparing the results obtained from three polymers featuring different side-groups: (**LD-PIAA**) no chromophores, (**P-PDI-1**) chromophores capable of π–π stacking, (**P-PDI-2**) chromophores where the stacking is hindered by the presence of bulky substituents in the bay area of the **PDI**. The effect of the different side chain functionalization on the macromolecule assembly at surfaces was explored by studying the morphology and aggregation tendency of all three polymers when adsorbed on silicon, mica and graphite substrates.

When deposited on a substrate, **P-PDI-1** molecules formed well defined bundles with a strong tendency of the molecules to supercoil. In particular, the major effect of stacking interactions between the PDI chromophores is to favor both inter-chain and intra-chain interactions, with the molecules tending to form well defined bundles and supercoils. The **LD-PIAAs** were found also to assemble into bundles of fibers through strong intra- and inter-molecular aggregation, although in this case no supercoiling was observed. In contrast, **P-PDI-2** was found to form shorter polymer strands and rounded structures, due to the absence of intermolecular interactions, caused by the sterically demanding side substituents.[30]

The results obtained indicate that, in multichromophoric polymers, the relationship between the central polymer backbone and the side functionalizations is not a simple ''master-slave''

interaction, in which the central backbone dictates the overall morphology forcing the pending perylene units to arrange themselves, only influencing the electronic properties of the material. Instead, the presence of side chain PDIs, and in particular their stacking behavior, plays a fundamental role in the material architecture, highlighted by the different self-assembling behavior of **P-PDI-1** from that of **P-PDI-2**.

Overall, the macromolecular conformation is dictated by a complex interplay between i) the covalent bonds of the polymer backbone, ii) the hydrogen bonding arrays between the amide units, and iii) the π–π interactions between the PDIs.

4. Solar Cells

In solar cells, the use of bulk hetero junction (BHJ) devices, in which acceptor and donor material are mixed to give maximal charge separation, represented a breakthrough in the field.[16] In these kinds of solar cell the high contact area between the two materials facilitates photogenerated excitons to successfully reach the interface between the acceptor and the donor. Preferably the interpenetration length should be on a length scale comparable to the mean exciton diffusion length, which amounts typically to 5–6 nm. Moreover the structures within the active layer should provide efficient pathways for the photogenerated charges to migrate to the corresponding electrodes and promote charge transport over charge recombination. Hence, the ''ideal'' blend for BHJ requires the combination of the following features: i) the electron-acceptor and -donor materials must be interpenetrating on the nm scale, thus phase separation on macroscopic scales must be hindered. ii) the electron–acceptor and –donor materials must form continuous paths to the electrodes, and charge accumulation or recombination in dead ends and bottlenecks needs to be prevented. iii) charge transport must be efficient with good charge mobility and low presence of structural defects within each phase. In the case of molecular materials, such properties can be achieved in highly crystalline systems exhibiting optimal overlap between stacked π–π orbitals to provide efficient charge hopping transport.

In the light of these rules of thumb, **P-PDI-1** appears to be an ideal model electron acceptor system to fabricate prototypical solar cells. To this end we have blended **P-PDI-1** with electron donors such as polythiophene- and polyfluorene-based conjugated polymers.[31] Prototypical devices with nominal (1:1) blend weight ratios of the polyisocyanide with poly(3-hexylthiophene) (**P3HT**) and poly(9,9′-dioctylfluorene-*co*-bis(*N*,*N*′-(4-butylphenyl))-bis(*N*,*N*′-phenyl)-1,4-phenyldiamine) (**PFB**) readily showed an order of magnitude improvement in power conversion efficiency, as compared to analogous blend using **M-PDI**, whereas the performance of strongly phase-separated **F8BT** (poly(9,9′-dioctylfluorene-*co*-benzothiadiazole) blend devices showed no such improvement.

In addition to the favorable phase separation and mixing of **P-PDI-1** blends with **P3HT** and **PFB**, as evidenced by AFM studies, the interpenetrating networks of **P-PDI-1** bundles offer an interesting means by which the connectivity of charge conduits back to the collecting electrodes may be improved. Commensurate improvements in both open-circuit voltage and short-circuit current, relative to analogous PDI-blend devices, have been observed. Additionally, we find that the quenching of photoluminescence (PL) in these photovoltaic blends of **P-PDI-1**, due to charge separation at the heterojunction interfaces, correlates very closely with the device efficiencies; the poorly performing **P-PDI-1**/**F8BT** blends show very low PL quenching efficiencies.

In order to obtain a greater insight in the relationship between this enhanced photovoltaic behavior and the architecture of the material, Atomic Force Microscopy investigations on the mixtures **P-PDI-1**:**P3HT** were carried out. These studies revealed that the two polymers form a continuous path of interpenetrated bundles, with no evidence of macroscopic phase separation, as observed in blends based on monomeric PDI.[20] To better clarify **P-PDI-1**:**P3HT** interactions on the nanometric scale, the same blend was also deposited in the form of ultrathin layers, where the single polymeric fibers can be resolved. Two different kinds of structures were observed (Fig. 2a): sparse, thick fibers (black arrow) surrounded by a denser network of thinner fibers (white arrow). Unfortunately, topography images do not offer information on the chemical composition of the observed features. Yet the surface potential map obtained by KPFM unambiguously reveals a clear difference in contrast between the two architectures (Fig. 2b). The surface potential (SP) of the thick fibers appears much more negative (darker in the KPFM image) than the silicon substrate, whereas the potential of the thin fibers is slightly more positive. The potential difference (∼30 mV) observed between the two structures, which arises from a partial transfer of charge between the two materials, indicates that the thick fibers are (mostly) composed of electron accepting **P-PDI-1** and the thin ones of electron donating **P3HT**. This bi-component motif exhibits a nanophase segregated character, with a high density of contact points between the electron accepting and donating phases.

By illuminating both **P-PDI-1**:**P3HT** blends with white light, a sudden change in the surface voltage was observed (Fig. 2e). Most significantly, an increase of the SP difference between acceptor and donor assemblies was observed revealing a photovoltaic effect occurring in **P-PDI-1**:**P3HT** aggregates with a resolution even down to the single **P3HT** strands. Figure 2b,d,f show the profiles obtained by tracing an arbitrary line in the corresponding three KPFM images in which we can distinguish both types of fibers (large and small) and substrate. The typical characteristic time scale of exciton splitting and charge generation are several orders of magnitude smaller than the time-resolution of the KPFM technique, i.e., a few ms. The measurements were however performed under steady-state conditions. During the illumination, charge generation and recombination cannot be monitored because both the deep and the shallow traps are continuously populated, hence, the measured SP values are an average of the charge density which does not reflect any time-dependence.

A clear and reproducible difference in the surface SP on such sub-monolayer thick films (Fig. 2) was observed upon turning on and off the light, highlighting the different behaviors between charging and de-charging. The surface potential measured at different points on the **P-PDI-1** fibers appeared to be uniform within experimental error, indicating a uniform level of charging of the material.[32]

Such a KPFM study on the nanoscale could for the first time give a direct insight into the correlation between surface potential

variations and molecular structure, through the direct visualization of the photovoltaic activity occurring in such a nanoscale phase segregated ultrathin film. The ability to obtain highly resolved and quantitative mapping of the photovoltaic activity on a nanoscale has a huge potential for gaining a greater understanding of the processes of charge separation and charge mobility in polymer chains.

Overall, the AFM and KPFM data measured on both thick and ultrathin layers show that thick films of **P-PDI-1** and **P3HT** exhibit architectures that are effectively phase-segregated yet interdigitated on the hundreds of nanometers scale, featuring both a high contact area between the two materials and well defined percolation paths for charges. This behavior is in contrast with that observed in **M-PDI:P3HT** ultrathin blends, in which crystal islands sit in a sea of P3HT.[33] This observation accounts for the results obtained macroscopically on the solar cells efficiency comparison.

This is crucial for the optimization of various fundamental photophysical properties of a functional bi-component macromolecular system, and ultimately for the improvement of the performances of any organic solar cell, e.g. its power conversion efficiency.

The obtained results on the electron-acceptor and electron-donor blends incorporating the **P-PDI-1** molecule provided evidence that the use of polyisocyanides as a molecular scaffold offers a great control over the morphology and connectivity of photovoltaic blends, leading to improved properties.

5. Field-Effect Transistors

To probe the intrinsic electrical characteristics of **P-PDI-1** films, and in particular their charge transport properties through the four helical stacks of perylene-bis(dicarboximide) (PDI) chromophores prototypes of bottom-gate field-effect transistors were fabricated and characterized. The **P-PDI-1** fibers were found to exhibit n-type electroactivity in thin films, with carrier mobilities in the order of 10^{-4} to 10^{-5} cm^2 V^{-1} s^{-1} at room temperature, rising to $\sim 10^{-3}$ cm^2 V^{-1} s^{-1} at 350 K, which are limited by inter-chain transport processes with significant activation energies. Such an electrical property is determined by the transfer of electrons through the π–π stack of PDIs. Conversely, **P-PDI-2**, in which π–π interactions were sterically hindered, exhibited much poorer device characteristics, as efficient intra-chain transport is inhibited. KPFM measurements of the work function of the P-PDIs nanostructures were in satisfactory agreement with electrochemical measurements of HOMO and LUMO levels from cyclic voltammetry. In particular, polymer **P-PDI-1** showed a much higher WF than either the polymer without PDIs (**LD-PIAA**) or the **P-PDI-2**. Theoretical modeling of the helical **P-PDI-1** system confirms that the charges can be transported efficiently through the 1D architecture.[35]

The electron transfer integrals between adjacent PDIs, calculated at the INDO quantum-chemical level on the basis of snapshots extracted from the molecular dynamics simulations, gave an average value of 350 $cm^{[1]}$. Compared to single crystals of small molecules such as the oligoacenes,[27] this is a significant value, which allows for efficient intramolecular electron transport along the polymer. However, because of positional disorder, the electronic couplings mediating electron transport showed a broad distribution. In particular, fluctuations of the rotation angles (around an equilibrium value of ~22°) between adjacent chromophores strongly influence the wavefunction overlap and the resulting transfer integral. We are now exploring molecular design strategies that reduce the average rotation angle to promote larger electronic communication between the PDIs.

It is however known that, while the highest charge mobilities in transistors have been obtained by employing single crystals of small

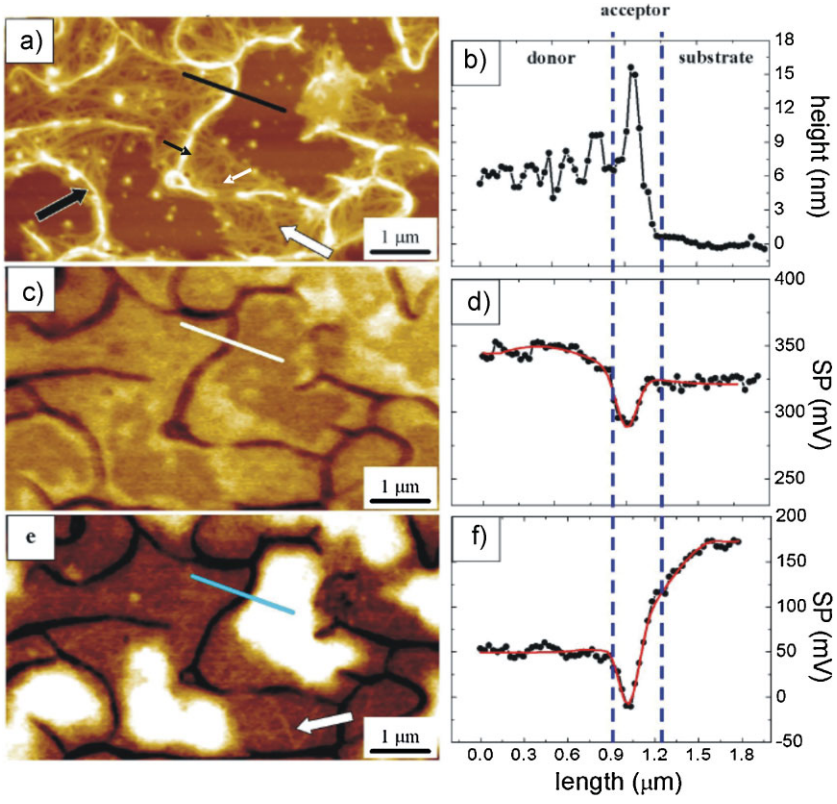

Figure 2. Potential maps of thin films of **P3HT** and **P-PDI-1** recorded with KPFM. a) AFM topography image of an ultrathin blend of **P-PDI-1** and **P3HT** deposited on silicon. c) Surface potential (SP) image of the same area as in (a) with no illumination, and e) under white light (~60 mW cm^{-2}) illumination. An overall negative potential shift upon light illumination is known to occur in these types of KPFM measurements, as previously reported for thick layers (see text): this is the reason why both **P-PDI-1** and **P3HT** appear more negative than the exposed bare silicon areas upon illumination. b,d,f) Measured (black lines and circles) and simulated (red lines) profiles obtained tracing an arbitrary line in the corresponding images (a), (c), and (e). Thus SP values depicted are the measured ones and therefore differ from the calculated asymptotical true values. Z-ranges: a) 32 nm, c) 120 mV, and e) 120 mV. Reprinted with permission from [32]. Copyright 2008, the American Chemical Society.

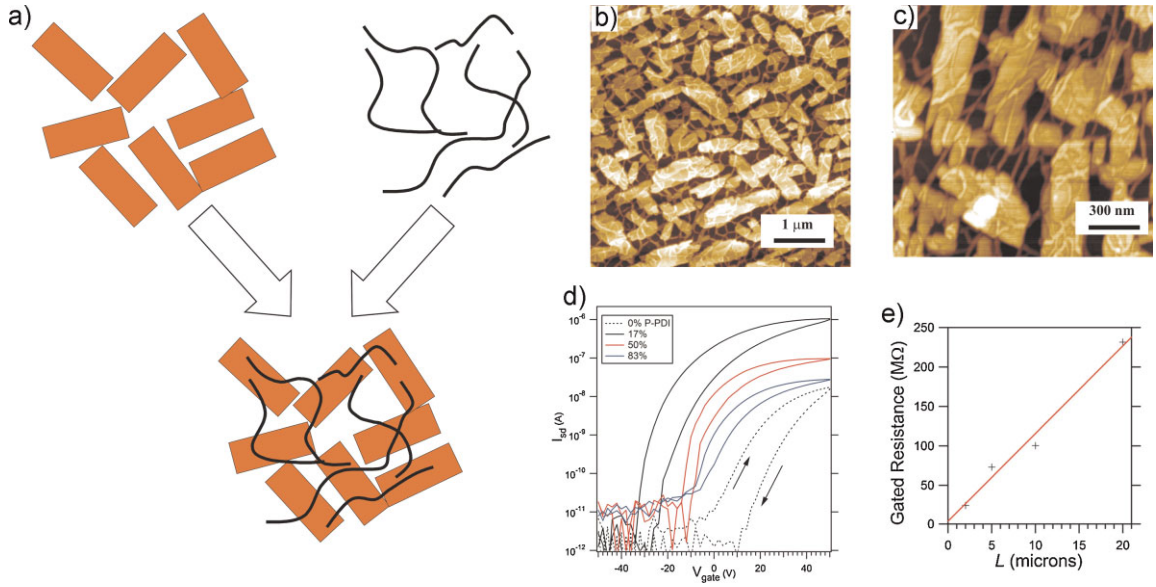

Figure 3. a) Schematic drawing of co-deposited **M-PDI** and **P-PDI-1** leading to polymer fibers bridging monomeric crystals. b,c) AFM topographical images of ultrathin film of blended monomeric **M-PDI** and **P-PDI-1** deposited from $CHCl_3$ on mica showing polymer fibers bridging monomeric crystals. d) Transfer characteristics, at a source-drain bias of 25 V, of **P-PDI-1:M-PDI** bottom-gate FETs with varying weight fractions of **P-PDI-1**, as indicated. The channel length and width was 2 and 10 000 μm, respectively, and the direction of gate-voltage sweep is indicated by the arrows. e) Gated resistance, defined as V_{sd}/I_{sd} at $V_{gate} = +50$ V, as a function of channel length (L), for the case of 17% **P-PDI-1**. The inferred contact resistance at L = 0 is 4.6 MΩ. Reprinted with permission from [33]. Copyright 2009, the American Chemical Society.

molecules as electroactive architectures,[36] typical devices are based on nano- or microcrystalline layers. In such systems the interfaces between different crystals act as bottlenecks for charge transport.[37] The generation of highly crystalline films featuring efficient percolation paths for charges is thus a crucial characteristic feature required to achieve elevated charge transport within an organic thin film. Monomeric PDIs forming polycrystalline films have been thoroughly employed as active layers in FETs.[18] To improve charge transport between the different crystals, an interesting strategy is to use flexible polymeric linkers, which can act as charge-carrying bridges between neighboring nanocrystals (Fig. 3a). This approach is similar to what occurs spontaneously in polythiophene semicrystalline layers, where a single polymeric chain can span many different neighboring nanocrystalline fibers or domains, thereby bridging them. In our specific case, **P-PDI-1** appeared as the ideal system to accomplish this goal. We therefore first investigated the self-assembly of bi-component films consisting of **M-PDI** and **P-PDI-1** co-deposited on SiO_x and mica substrates from solution. The morphology of these bi-component films was characterized by AFM. The studies revealed that monomer-polymer interactions can be controlled by varying solvent and/or substrate polarity, so that either the monomer packing dictates the polymer morphology or vice versa, leading to a morphology in which **M-PDI** nanocrystals are connected with each other by **P-PDI-1** polymer wires (Fig. 3b,c).[34]

KPFM analysis on the nanoscale showed minimal differences in surface potential between the two phases, which suggests a low potential barrier for charge transport. Compared to pure **M-PDI** or **P-PDI-1** films, bi-component films containing 17% of polymer, possess polymer interconnections between crystallites of the monomer and display a significant improvement in electrical connectivity and a two orders of magnitude increase in charge carrier mobility within the film, as measured in FET devices (Fig. 3d,e).[34]

Our technique based on the controlled formation of percolation pathways for charge transport through the use of **P-PDI-1** fibers offers an attractive strategy to improve the performance of electronic devices based on semiconducting polycrystalline films, without the formation of prohibitive charge-trapping sites or injection barriers at the connection points. The strategy presented here for promoting charge transport in polycrystalline films for organic electronics is not limited to PDI electroactive derivatives, and can be more generally applied to any combination of a small electroactive molecule and its polymeric analogue that is linked to a rigid scaffold, including high performance molecular moieties such as thiophenes or polyfluorenes.

6. Conclusions and Outlook

We have devised a new strategy based on a polyisocyanide scaffold to achieve control over the position of functional molecular units, with a precision on the sub-ångström scale, up to a length scale of several hundreds of nanometers. The main features of the scaffold can be summarized as follows.

i) it has a highly rigid architecture, which adopts a helical conformation when bulky groups are attached to its backbone;
ii) it possesses chiral alanine side chains, which interact through hydrogen bonding, not only allowing the backbone to adopt a 4_1 (four repeats per turn) helical conformation with a preferred handedness, but also providing greater rigidity and stability to the polymer;

iii) it has small flexible linkers between the chromophores and the polymer backbone, making it possible to the chromophores to remain close to the polymeric chain, but simultaneously allows them to orientate themselves on a molecular scale to maximize their π–π interactions;
iv) it contains aromatic chromophores, which provides the electronic and optical functions to the architecture, and finally
v) it possesses flexible alkyl chains, which offer increased solubility in organic solvents. The combination of these features results in macromolecules possessing extremely high rigidity, good solution processability, and the capacity to generate and transport charges. The macromolecules moreover have a high molecular weight.

The use of rigid polymer chains as scaffolds to control the position of electroactive moieties is not limited to PDI chromophores attached to polyisocyanides, and a wide variety of ultra-stiff nanowires based on different functional groups is accessible.[22] The possibility to tune independently, by chemical modification, the mechanical properties of the polymer, i.e., the rigidity of the wire (on the nanometers scale), the linker flexibility and the functional group stacking (on the molecular scale) will add a new class of materials with much improved mechanical and electronic properties to the continuously growing toolbox of nanoelectronics. By exploiting the click-chemistry approach in a modular fashion, the covalent attachment of various building blocks of interest for solar cell (e.g., C60s) or transistor (e.g., pentacene) applications is conceivable. Intriguingly, at the single molecule level, the presence of cumulative local dipoles along the backbone generates an electric field resulting in an energy gradient for charge migration. **P-PDI-1** might thus be an interesting candidate for single molecule rectification. It is worth noting that the use of a flexible spacer connecting the stiff polymer backbone to the electronic functional unit (i.e., PDI) grants to the system a certain degree of conformational freedom that allows the PDI stacking to occur, ultimately providing an electronic function to the architecture.

Overall, as an alternative to the use of supramolecular scaffolds for controlling the position of functional units in space (in particular in 2D),[38] our macromolecular scaffolding strategy appears to be highly suitable to explore the relationship between architecture and function in molecular materials, not only for electronics, but also for catalysis and medicine.

Acknowledgements

This work was supported by the ESF-SONS2-SUPRAMATES, by the EU through the Marie Curie projects ITN-SUPERIOR (PITN-GA-2009-238177) and RTN-THREADMILL (MRTN-CT-2006-036040), the EC FP7 ONE-P large-scale project no. 212311, by the NanoSci-E+ project SENSORS, by the Regione Emilia-Romagna PRIITT Prominer Net-Lab and by the International Center for Frontier Research in Chemistry (FRC). The work in Mons is partly supported by the Interuniversity Attraction Pole program of the Belgian Federal Science Policy Office (PAI 6/27) and by FNRS-FRFC. DB is research director of FNRS. ST acknowledges a grant from FRIA, and R.J.M.N. from the Royal Netherlands Academy of Science. C.E.F. thanks the Leverhulme Trust (UK) for an ''Early Career Fellowship''.

Published online: January 4, 2010

[1] a) Special issue on ''Supramolecular Approaches to Organic Electronics and Nanotechnology'', *Adv. Mater.* **2006**, *18*, 1227. b) Special issue on ''Functional Supramolecular Architectures'', *Adv. Mater.* **2009**, *21*, 1027. c) V. Palermo, P. Samorì, *Angew. Chem. Int. Edit.* **2007**, *46*, 4428. d) A. Schenning, E. W. Meijer, *Chem. Commun.* **2005**, 3245.
[2] R. H. Friend, R. W. Gymer, A. B. Holmes, J. H. Burroughes, R. N. Marks, C. Taliani, D. D. C. Bradley, D. A. Dos Santos, J. L. Brédas, M. Logdlund, W. R. Salaneck, *Nature* **1999**, *397*, 121.
[3] a) S. Sergeyev, W. Pisula, Y. H. Geerts, *Chem. Soc. Rev.* **2007**, *36*, 1902. b) J. S. Wu, W. Pisula, K. Müllen, *Chem. Rev.* **2007**, *107*, 718.
[4] a) F. J. M. Hoeben, P. Jonkheijm, E. W. Meijer, A. Schenning, *Chem. Rev.* **2005**, *105*, 1491. b) P. Samorì, J. P. Rabe, *J. Phys. Condens. Matter* **2002**, *14*, 9955.
[5] a) Special issue on ''Supramolecular Chemistry and Self-Assembly'', *Science* **2002**, *295*, 2396. b) Special issue on ''Supramolecular Chemistry and Self-Assembly'', *Proc. Nat. Acad. Sci. U.S.A.* **2002**, *99*, 4762. c) Special issue on ''Supramolecular Chemistry Anniversary'', *Chem. Soc. Rev.* **2007**, *36*, 125.
[6] M. Cavallini, P. Stoliar, J. F. Moulin, M. Surin, P. Leclere, R. Lazzaroni, D. W. Breiby, J. W. Andreasen, M. M. Nielsen, P. Sonar, A. C. Grimsdale, K. Mullen, F. Biscarini, *Nano Letters* **2005**, *5*, 2422.
[7] M. B. J. Otten, C. Ecker, G. A. Metselaar, A. E. Rowan, R. J. M. Nolte, P. Samorì, J. P. Rabe, *Chem. Phys. Chem.* **2004**, *5*, 128.
[8] a) B. W. Messmore, J. F. Hulvat, E. D. Sone, S. I. Stupp, *J. Am. Chem. Soc.* **2004**, *126*, 14452. b) L. Sardone, V. Palermo, E. Devaux, D. Credgington, M. De Loos, G. Marletta, F. Cacialli, J. Van Esch, P. Samorì, *Adv. Mater.* **2006**, *18*, 1276.
[9] I. O. Shklyarevskiy, P. Jonkheijm, N. Stutzmann, D. Wasserberg, H. J. Wondergem, P. C. M. Christianen, A. P. H. J. Schenning, D. M. de Leeuw, Z. Tomovic, J. S. Wu, K. Müllen, J. C. Maan, *J. Am. Chem. Soc.* **2005**, *127*, 16233.
[10] J. J. L. M. Cornelissen, J. J. J. M. Donners, R. de Gelder, W. S. Graswinckel, G. A. Metselaar, A. E. Rowan, N. A. J. M. Sommerdijk, R. J. M. Nolte, *Science* **2001**, *293*, 676.
[11] P. Samorì, C. Ecker, I. Goessl, P. A. J. de Witte, J. J. L. M. Cornelissen, G. A. Metselaar, M. B. J. Otten, A. E. Rowan, R. J. M. Nolte, J. P. Rabe, *Macromolecules* **2002**, *35*, 5290.
[12] F. Cacialli, J. S. Wilson, J. J. Michels, C. Daniel, C. Silva, R. H. Friend, N. Severin, P. Samorì, J. P. Rabe, M. J. O'Connell, P. N. Taylor, H. L. Anderson, *Nat. Mater.* **2002**, *1*, 160; S. R. Forrest, *Nature* **2004**, *428*, 911.
[13] a) M. Mas-Torrent, C. Rovira, *Chem. Soc. Rev.* **2008**, *37*, 827. b) A. R. Murphy, J. M. J. Fréchet, *Chem. Rev.* **2007**, *107*, 1066. c) H. Sirringhaus, *Adv. Mater.* **2005**, *17*, 2411. d) J. Zaumseil, H. Sirringhaus, *Chem. Rev.* **2007**, *107*, 1296.
[14] M. Muccini, *Nat. Mater.* **2006**, *5*, 605.
[15] J. Jang, *Mater. Today* **2006**, *9*, 46.
[16] a) J. J. M. Halls, C. A. Walsh, N. C. Greenham, E. A. Marseglia, R. H. Friend, S. C. Moratti, A. B. Holmes, *Nature* **1995**, *376*, 498. b) G. Yu, J. Gao, J. C. Hummelen, F. Wudl, A. J. Heeger, *Science* **1995**, *270*, 1789.
[17] a) C. W. Struijk, A. B. Sieval, J. E. J. Dakhorst, M. van Dijk, P. Kimkes, R. B. M. Koehorst, H. Donker, T. J. Schaafsma, S. J. Picken, A. M. van de Craats, J. M. Warman, H. Zuilhof, E. J. R. Sudholter, *J. Am. Chem. Soc.* **2000**, *122*, 11057. b) F. Würthner, *Chem. Commun.* **2004**, 1564. c) J. Elemans, R. Van Hameren, R. J. M. Nolte, A. E. Rowan, *Adv. Mater.* **2006**, *18*, 1251. d) F. Nolde, W. Pisula, S. Muller, C. Kohl, K. Müllen, *Chem. Mater.* **2006**, *18*, 3715.
[18] a) A. L. Briseno, S. C. B. Mannsfeld, C. Reese, J. M. Hancock, Y. Xiong, S. A. Jenekhe, Z. Bao, Y. Xia, *Nano Lett.* **2007**, *7*, 2847. b) Y. K. Che, A. Datar, K. Balakrishnan, L. Zang, *J. Am. Chem. Soc.* **2007**, *129*, 7234. c) H. N. Tsao, W. Pisula, Z. H. Liu, W. Osikowicz, W. R. Salaneck, K. Müllen, *Adv. Mater.* **2008**, *20*, 2715.

[19] J. J. Dittmer, R. Lazzaroni, P. Leclère, P. Moretti, M. Granstrom, K. Petritsch, E. A. Marseglia, R. H. Friend, J. L. Brédas, H. Rost, A. B. Holmes, *Sol. Energy Mater. Sol. Cells* **2000**, *61*, 53.
[20] L. Schmidt-Mende, A. Fechtenkötter, K. Müllen, E. Moons, R. H. Friend, J. D. MacKenzie, *Science* **2001**, *293*, 1119.
[21] E. Schwartz, V. Palermo, C. E. Finlayson, Y.-S. Huang, M. B. J. Otten, A. Liscio, S. Trapani, I. González-Valls, P. Brocorens, J. J. L. M. Cornelissen, K. Paneva, K. Müllen, F. Spano, R. H. Friend, D. Beljonne, R. J. M. Nolte, P. Samorì, A. E. Rowan, *Chem. Eur. J.* **2009**, *15*, 2536.
[22] P. A. J. de Witte, M. Castriciano, J. Cornelissen, L. M. Scolaro, R. J. M. Nolte, A. E. Rowan, *Chem. Eur. J.* **2003**, *9*, 1775.
[23] D. M. Vriezema, J. Hoogboom, K. Velonia, K. Takazawa, P. C. M. Christianen, J. C. Maan, A. E. Rowan, R. J. M. Nolte, *Angew. Chem. Int. Ed.* **2003**, *42*, 772.
[24] V. V. Rostovtsev, L. G. Green, V. V. Fokin, K. B. Sharpless, *Angew. Chem. Int. Ed.* **2002**, 2596.
[25] E. Schwartz, H. J. Kitto, R. de Gelder, R. J. M. Nolte, A. E. Rowan, J. J. L. M. Cornelissen, *J. Mater. Chem.* **2007**, *17*, 1876.
[26] H. J. Kitto, E. Schwartz, M. Nijemeisland, M. Koepf, J. J. L. M. Cornelissen, A. E. Rowan, R. J. M. Nolte, *J. Mater. Chem.* **2008**, *18*, 5615.
[27] Y. C. Cheng, R. J. Silbey, D. A. da Silva Filho, J. P. Calbert, J. Cornil, J.-L. Brédas, *J. Chem. Phys.* **2003**, *118*, 3764.
[28] S. Westenhoff, C. Daniel, R. H. Friend, C. Silva, V. Sundstrom, A. Yartsev, *J. Chem. Phys.* **2005**, *122*, 094903.
[29] C. Daniel, S. Westenhoff, F. Makereel, R. H. Friend, D. Beljonne, L. M. Herz, S. C., *J. Phys. Chem. C* **2007**, *111*, 19111.
[30] V. Palermo, E. Schwartz, A. Liscio, M. Otten, B.J., K. Müllen, R. J. M. Nolte, A. E. Rowan, P. Samorì, *Soft Matter* **2009**, *5*, 4680.
[31] S. Foster, C. E. Finlayson, P. E. Keivanidis, Y.-S. Huang, I. Hwang, R. H. Friend, M. B. J. Otten, L.-P. Lu, E. Schwartz, R. J. M. Nolte, A. E. Rowan, *Macromolecules* **2009**, *42*, 2023.
[32] V. Palermo, M. B. J. Otten, A. Liscio, E. Schwartz, P. A. J. de Witte, M. A. Castriciano, M. M. Wienk, F. Nolde, G. De Luca, J. J. L. M. Cornelissen, R. A. J. Janssen, K. Müllen, A. E. Rowan, R. J. M. Nolte, P. Samorì, *J. Am. Chem. Soc.* **2008**, 2008. 14605.
[33] A. Liscio, G. De Luca, F. Nolde, V. Palermo, K. Müllen, P. Samorì, *J. Am. Chem. Soc.* **2008**, *130*, 780.
[34] R. Dabirian, V. Palermo, A. Liscio, E. Schwartz, M. B. J. Otten, C. E. Finlayson, E. Treossi, R. H. Friend, G. Calestani, K. Müllen, R. J. M. Nolte, A. E. Rowan, P. Samorì, *J. Am. Chem. Soc.* **2009**, *131*, 7055.
[35] C. E. Finlayson, R. H. Friend, M. B. J. Otten, E. Schwartz, R. J. M. Nolte, A. E. Rowan, V. Palermo, A. Liscio, P. Samorì, K. Paneva, K. Müllen, S. Trapani, D. Beljonne, *Adv. Funct. Mater.* **2008**, *18*, 3947.
[36] V. C. Sundar, J. Zaumseil, V. Podzorov, E. Menard, R. L. Willett, T. Someya, M. E. Gershenson, J. A. Rogers, *Science* **2004**, *303*, 1644; J. Takeya, M. Yamagishi, Y. Tominari, R. Hirahara, Y. Nakazawa, T. Nishikawa, T. Kawase, T. Shimoda, S. Ogawa, *Appl. Phys. Lett.* **2007**, *90*.
[37] a) P. Annibale, C. Albonetti, P. Stoliar, F. Biscarini, *J. Phys. Chem. A* **2007**, *111*, 12854. b) K. Puntambekar, J. P. Dong, G. Haugstad, C. D. Frisbie, *Adv. Funct. Mater.* **2006**, *16*, 879. c) J. Zhang, J. P. Rabe, N. Koch, *Adv. Mater.* **2007**, *20*, 3254.
[38] G. P. Spada, S. Lena, S. Masiero, S. Pieraccini, M. Surin, P. Samorì, *Adv. Mater.* **2008**, *20*, 2433.